Journal of Molecular Structure: THEOCHEM 946 (2010) 83–87

Contents lists available at ScienceDirect

Journal of Molecular Structure: THEOCHEM

journal homepage: www.elsevier.com/locate/theochem

Structure of the interface between water and self-assembled monolayers of neutral, anionic and cationic alkane thiols

Borys Szefczyk [a,b,*], Ricardo Franco [c], José A.N.F. Gomes [a], M. Natália D.S. Cordeiro [a,*]

[a] REQUIMTE, Department of Chemistry, Faculty of Science, University of Porto, Rua do Campo Alegre 687, 4169-007 Porto, Portugal
[b] Institute of Physical and Theoretical Chemistry, Wrocław University of Technology, Wybrzeże Wyspiańskiego 27, 50-370 Wrocław, Poland
[c] REQUIMTE, Department of Chemistry, Faculty of Science and Technology, New University of Lisbon, 2829-516 Caparica, Portugal

ARTICLE INFO

Article history:
Received 15 July 2009
Received in revised form 6 November 2009
Accepted 12 November 2009
Available online 17 November 2009

Keywords:
Dipole moment
Surface
Gold (111)
Gromacs
Tilt angle

ABSTRACT

Molecular dynamics simulations of self-assembled monolayers (SAMs) of alkanethiol derivatives interfaced with water reveal the structure of the interface and show how it influences the properties of water. Three SAMs of different character (neutral, anionic and cationic) are compared: 6-hexanethiol, 11-mercaptoundecanoic acid and 11-amino-1-undecanethiol. The simulation captures phenomena such as the hydrophobic gap, local increase of the density of water near the interface and ordering of water into layers.

1. Introduction

Thiol-terminated alkanes of varying length can be chemically attached to the surface of noble metals [1]. These organic molecules are able to arrange into densely packed monolayers—so called self-assembled monolayers (SAMs). Commonly, gold is used as the substrate, but silver, platinum, copper and other metals have also been used, as well as non-metallic surfaces [1,2]. Such monolayers form very stable and regular surfaces and the metal enhances the range of applications, so that various electrochemical devices and sensors can be built and used for measuring concentration of specific ions (e.g. by introducing crown ethers as the functional groups), biomolecules like specific sequences of DNA (by a prior deposition of complementary nucleotides) or ligand-binding proteins (e.g. enzymes, by using SAMs with a chemically bound ligand) [3]. Carefully chosen dipolar monolayer of molecules can modify the work function of the electrode, so that the energy barrier for the electron extraction or injection is decreased, which in turn decreases the voltage necessary to activite the device [4]. Gold nanoparticles can also be functionalized with thiolated alkanes monolayers; such species can by used for example as drug carriers or markers for the diseased tissues, when the nanoparticle has been equipped with ligands which can bind to receptors displayed on the surface of the 'ill' cells [5]. The SAMs constitute also a model which can mimic a biological membrane [1]. Particularly interesting topic is the interaction of SAMs with enzymes, as deposition of enzymes on the surface of the SAM opens a broad range of applications involving biosensing and controlling enzymatically catalysed reactions [3]. On the other hand, the SAMs are also applied to protect the surface from the protein adsorption [6], namely via biocompatible oligo(ethylene glycol) and poly(ethylene glycol) moieties—such versatility of applications being possible thanks to the functional groups introduced into the SAM. Depending on the purpose, the alkane molecules will present different chemical functionalizations. This functionalization can be achieved, for example, by adding anionic, cationic or neutral substituents. However, up to date, there is no deeper understanding of the physics of the processes at the surface, since the structure of the interface is not well understood; what is clear, is that the properties of the solvent (typically water) next to the interface are different from the bulk properties [6]. Large concentration of specific groups in almost perfect, lateral structure can influence greatly the characteristics of the solvent in contact with the surface. Crystal structure of the surface can induce, in principle, similar organization of the solvent ("ice-like" water) [7]. Several types of SAMs have been investigated so far, using experimental methods and molecular simulations. Most commonly investigated are alkanethiols of different length [8–10], hydroxy-terminated alkanes and poly(glycols) [11], and carboxylic acids [12,13]. The carboxylic acids can deprotonate, which constitutes another challenge, since the pK_a of the molecules packed into

* Corresponding author. Tel.: +351 226082802; fax: +351 226082959.
E-mail addresses: borys.szefczyk@fc.up.pt (B. Szefczyk), r.franco@dq.fct.unl.pt (R. Franco), jfgomes@fc.up.pt (J.A.N.F. Gomes), ncordeir@fc.up.pt (M.N.D.S. Cordeiro).

0166-1280/$ - see front matter © 2009 Elsevier B.V. All rights reserved.
doi:10.1016/j.theochem.2009.11.021

a dense monolayer is very different from the aqueous solution [14]. Usually, the carboxyl-terminated SAMs are studied at very low pH, where the layer is completely protonated. However, at high pH the charge of the monolayer has to be counterbalanced by ions (hydronium or salt). This rises another issue—the problem where are the counterions; if they stay close to the surface or diffuse into the solvent. Bearing this thoughts in mind, the present work focuses on the properties of the interface between water and three model systems: monolayer of 1-hexanethiol (HXT), monolayer of 11-mercaptoundecanoic acid (MUA) and monolayer of 11-amino-1-undecanethiol (AUT, Fig. 1) assembled into monolayer onto a gold (111) surface. These systems, display on the surface hydrophobic, anionic and cationic groups, respectively, therefore, affecting the structure of water in a different manner. The simulations are performed at pH 8, ensuring stability of proteins such as the ferrochelatase [15]. At this pH the MUA monolayer is deprotonated and the AUT monolayer is protonated, being the charge of each counterbalanced by ions.

2. Methods

According to experimental results [1], the alkanethiols form a densely packed layer, arranged into $(\sqrt{3}\times\sqrt{3})R30^\circ$ lattice. The experimental lattice constant of gold, used in these calculations is 2.88 Å. It has been disputed, if the alkanethiols adsorb in the bridge, on-top or threefold position. Theoretical works indicate that the sulphur atom occupies the bridge [16,17] and the threefold binding site [18,19], whereas experimental works suggest an on-top binding site [20,21]. Recently, it has been found, that the binding of alkanethiols proceeds with a significant surface reconstruction, including formation of an S–Au–S bridge [22,23]. In the present work, in order to avoid problems with ambiguous parametrization of the gold–SAM interactions and to simplify the calculations, the surface of the metal is omitted in the calculations. Instead, the sulphur atoms are fixed in space using harmonic constraints with force constant of 50 MJ mol^{-1} nm^{-2}. Such approximation does not imply any specific adsorption site, but merely ensures that the $(\sqrt{3}\times\sqrt{3})R30^\circ$ arrangement of the molecules is preserved. It is widely acknowledged, that the alkanethiols are chemically adsorbed, i.e. the thiol group is dissociated and sulphur binds to the gold surface. The united-atom GROMOS96 force field [24] is used to calculate the potential energy and forces. United-atom force fields were also used in other simulations of SAMs [13], although some authors suggest that in a densely packed monolayers the explicit description on hydrogens in the aliphatic chain might be necessary [25]. In our calculations, since the gold surface is not explicitly included, the alkanethiols are terminated with the methyl group (which in the united-atom formulation of the GROMOS96 force field is just a single atom). Compared to a hydrogen atom, the terminating methyl group is heavier and therefore, more convenient to simulate (i.e. allows for a larger time step). The following procedure was applied to simulate the SAMs: HXT, MUA and AUT were build and multiplied on a $(\sqrt{3}\times\sqrt{3})R30^\circ$ lattice with a lattice constant of 2.88 Å. In all three cases, the unit cell contained 19×11 molecules resulting in a roughly square box of 94.43×94.60 Å. The initial height of the simulation box was set to 50 Å (along the z direction), to ensure separation between periodic images, since the periodic boundary conditions (PBC) were applied to all directions. The SAMs were positioned at the bottom of the simulation box, with sulphur atoms at z coordinate equal to 2 Å. Afterwards, the box was filled with 'simple point charge' (SPC) water molecules [26]. It was assumed, that the model should correspond to pH 8, and therefore, the MUA was completely deprotonated and AUT was constructed as a mixed monolayer of neutral and protonated molecules. The ratio of protonated to neutral molecules was chosen based on experimental values of local pK_a: 5.0 and 8.9 for carboxylic and amine SAM, respectively [14]. HXT and MUA contained 418 identical molecules, whereas AUT contained 371 protonated molecules (11-ammonium-1-undecanethiol) and 47 neutral molecules (11-amino-1-undecanethiol). The position of 47 neutral molecules in the AUT surface was chosen so as to spread them uniformly between the charged molecules. The charge of MUA and AUT monolayers was counterbalanced by adding a layer of counterions: sodium (Na^+) in case of MUA and chloride (Cl^-) in case of AUT. The number of ions was equal to the number of charged molecules and each ion was placed initially over the sulphur atom of a respective molecule at z coordinate equal to 20 Å. For the neutral HXT SAM, both, sodium and chloride ions were added (31 + 31 ions) to ensure total salt concentration of ca. 0.15 M. All geometry optimizations and MD simulations have been performed in GROMACS 4 package [27]. In order to allow for the relaxation of the initial model, a partial optimization was performed, with constrains on atoms other than hydrogens. The optimization was done using the Steepest Descent method until the maximum force has reached 2000 kJ mol^{-1} nm^{-1}. Next, the system was simulated by performing the Np$_z$T molecular dynamics over 10 ns, with a time step of 2 fs. Np$_z$T ensemble (meaning that the pressure control was done only along the z direction) was used to allow for the box size relaxation in the direction perpendicular to the surface of SAM. The size of the box in the x and y directions was maintained constant. The temperature was kept at 300 K using the Nosé–Hoover thermostat [28,29] and the pressure along the z direction was controlled using the Parrinello–Rahman barostat [30]. The bond lengths were constrained using the LINCS algorithm [31].

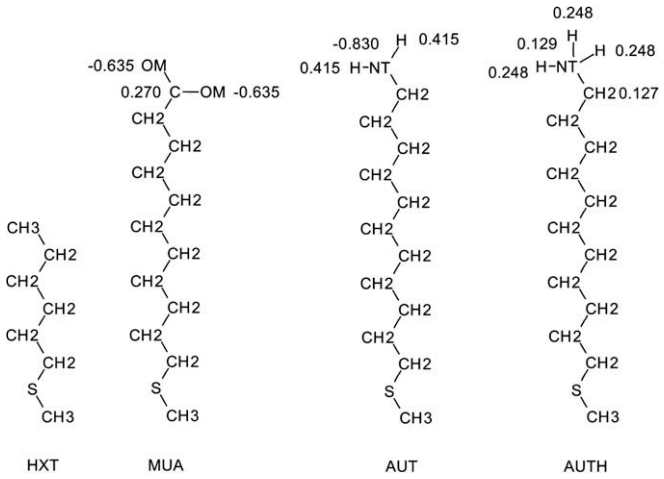

Fig. 1. The GROMOS96 force field parameters applied to the alkanethiol molecules. Atom types and charges (if different than zero) are shown.

A second simulation of AUT was set up, with a box significantly elongated in the z direction, to verify how the results are affected by using PBC. The simulation was performed in exactly the same way, except that the unit cell size was $49.7\times51.6\times200$ Å and contained 10×6 molecules of aminoundecanethiol in protonation state corresponding to pH 8. This model will be referred to as AUT2.

HXT, MUA and AUT are non-standard residues, however the building blocks of these molecules are present in GROMOS96 force field. Therefore, in the simulations of SAMs, the existing parameters were used. In Fig. 1, the charges and atom types are shown. The bonding parameters and topology was based on functional groups of amino acids: glutamate (MUA), lysine (AUT) and methionine (sulphur parameters).

In the simulations of HXT and MUA, initial 2 ns were treated as equilibration phase and the period 2–10 ns was used to collect the

statistics. In AUT, the interactions between SAM, water and ions did not fully stabilize until 15 ns, therefore, the run was extended and statistics were collected between 15 and 23 ns. In AUT2 the production run spans from 12 to 20 ns. In all cases the equilibration period was defined by the time needed to stabilize the interaction energy between SAM and water or ions. The simulations results are analysed by calculating the tilt and precession angles (see Fig. 2 for definition), the thickness of the monolayer and mass distribution along the axis perpendicular to the surface. In order to analyse the structure of the interface, the density profiles of water, SAM and ions are plotted along the z axis, as well as the z component of the dipole moment.

3. Results and discussion

On a clean, flat surface of gold (111), the adsorbed molecules bind in a $(\sqrt{3}\times\sqrt{3})R30^\circ$ lattice, which determines the structure of the whole SAM. The monolayer can be tilted, so that the thickness is not simply equal to the length of the chain. Thickness of the SAM can be measured experimentally, by ellipsometry [8], surface plasmon resonance [10] or X-ray photoelectron spectroscopy [32]. Linear dependencies between the length and the thickness have been established [8,33,34], however, depending on the method used, the values reported differ significantly. For example, the experimental thickness of a MUA SAM is between 15.5 and 19 Å depending on the method used [10,12]. Even in the theoretical description the parameters can be ambiguous, therefore the definition shown in Fig. 2 should be consulted when comparing with results from other sources. In Table 1 properties of SAMs are collected. As shown by Duffy and Harding [35] the tilt angle may depend on the arrangement of the molecules constituting the SAM, on the temperature and if the surface is dry or wet. At pH 8, which was assumed in the simulations, the MUA should be completely deprotonated, whereas the AUT would be protonated in 89%. The negative charge of MUA and positive charge of AUT layer is counterbalanced by ions (Cl^- and Na^+ in this case) which form a stable layer on top of the SAM (Figs. 4 and 5). Duffy and Harding have studied system composed of 16-mercaptohexadecanoic acid containing calcium ions and found that the ions form a slab on top of the SAM [35].

The SAMs exhibit a tilt of the alkyl chain, which results from the arrangement of the SAM on the gold (111) surface. HXT is tilted by 24° from the z axis, MUA and AUT by 26° and 21°, respectively (Table 1). This results in an effective thickness of the monolayer, which is 7.0 Å in case of HXT, 13.4 Å in MUA and 13.9 Å in AUT. Even if the Au–S distance is added (not included in these figures), the thickness of MUA is still closer to the experimental value of 15.5 Å, reported by Damos et al. [10], than the 19.0 Å, reported by Chidsey and Loiacono [12]. The arrangement of SAM on top of the gold surface determines also the precession angle (χ). Histograms of χ are shown in Fig. 3. HXT adopts orientation called *nearest-neighbour* (NN) [36], which in this model corresponds to $\chi = 0, 60, 120$ etc. MUA orientates to the *next-nearest-neighbour* (NNN, $\chi = 30, 90, 150$ etc.), whereas AUT is typically oriented between NN and NNN configurations. Coexistence of differently oriented domains is not observed, but this may be because the model is not large enough.

Near the surface of the SAM, the properties of water are altered significantly, compared to bulk liquid under normal condition. Fig. 4 shows the density profile of water together with the average value of the z-component of the dipole moment. In each of the SAMs, there is a gap of decreased density just above the surface, followed by a peak of increased density, decaying in an oscillatory manner. For the hydrophobic HXT, the gap spanning between the terminal methyl group of SAM and first peak of water density is ca. 3.5 Å wide. Within this gap, the total density drops almost to zero. Smaller gaps are observed in MUA (2.7 Å) and AUT (3.3 Å). Also, in the hydrophilic SAMs, the total density does not diminish completely. The local increase of the density of water can reach the value of 1636 kg m^{-3} in MUA, but only 1222 and 1217 kg m^{-3} in HXT and AUT, respectively. However, this values can be somewhat overestimated, due to the long-range interactions, as explained below. The so called "hydrophobic gap" was observed before, in capacitance measurements [37], neutron reflectivity experiments [11] and predicted in molecular simulations [13,38,39].

The increased density is connected with different orientation of the water molecule near the interface. The ordering of water molecules can be seen by investigating the average value of the z component of the dipole moment, which for bulk water is expected to be zero. Fig. 4 shows that the dipole moment oscillates in the same way as the density does, meaning that the interface is covered with approximately monomolecular layers of water oriented in opposite directions. In MUA, the first layer has very low density, but $D_z = -1.5$ D—close to the total dipole moment of water, so almost all molecules are arranged with hydrogens facing the SAM. The next layer, which also coincides with a maximum of the density, is less organized, but there is a clear preference for the hydrogens to point away from the surface. It is interesting to observe that in HXT, the oscillations in D_z are also present. The point charges on atoms of HXT are all zero, so the orientation must stem entirely from the behaviour of water at the interface and not from the electrostatic interaction. Unexpectedly, the AUT SAM appears to be very different from HXT and MUA. In the latter two, at the

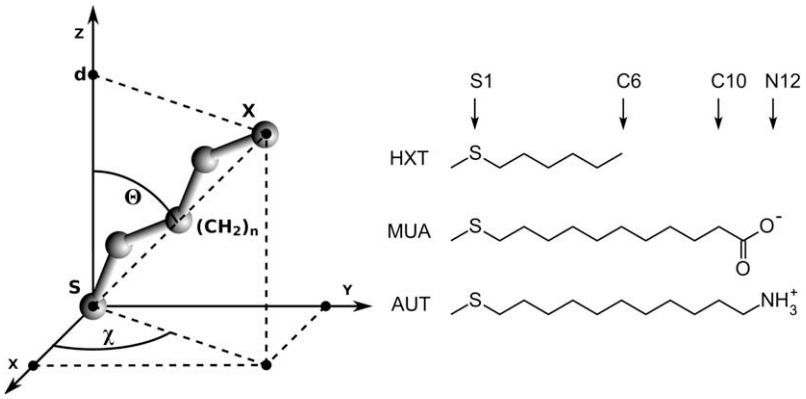

Fig. 2. Definition of the tilt angle (Θ), precession angle (χ) and monolayer thickness (d). S means the sulphur S1 atom and X is C6, C10 and N12 (in HXT, MUA and AUT, respectively). The angles are measured between the z axis and line joining sulfur (S1) and C6 (HXT), C10 (MUA) and N12 (AUT). The thickness in measured between S1 and C6 (HXT), top oxygen (MUA) and N12 (AUT).

Table 1
Thickness and tilt angle of the SAMs. See Fig. 2 for definition of the parameters.

	HXT	MUA	AUT
Thickness (d, Å)	7.0	13.4	13.9
Thickness RMSD (Å)	0.3	0.4	0.6
Tilt angle (Θ, deg.)	24	26	21
Tilt angle RMSD (deg.)	5.1	3.8	4.8

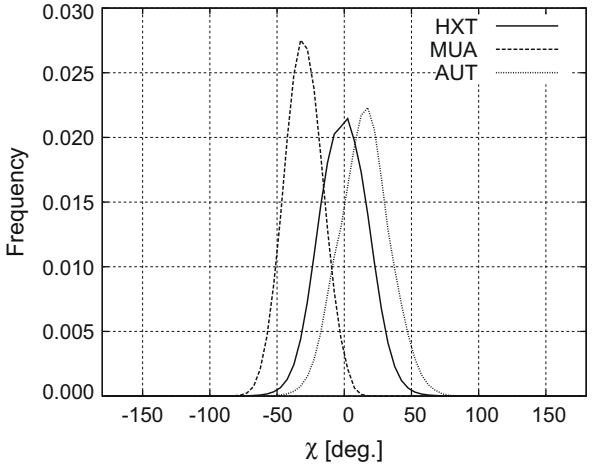

Fig. 3. Histogram of the precession angle χ in the monolayers of HXT, MUA and AUT.

interface, the z component of the dipole moment of water oscillates between positive and negative values, which means layers of water oriented in opposite directions. In AUT, there are 2–3 layers of water, which display positive D_z, separated by layers of unoriented water (D_z close to zero). The influence of AUT monolayer reaches much deeper into the solvent than the influence of HXT or MUA and a small, but constant decrease of D_z of the water can be observed. This would explain why the equilibration of AUT took 15 ns, whereas HXT and MUA have equilibrated in less than 2 ns. Naturally, this also means that the separation of periodic images by 50 Å might be insufficient. This difference in the dipole moment profile could be explained by the fact that in MUA, the ions are tightly bound to the SAM: in the slab of bulk water between $z = 25$ Å and $z = 35$ Å there is on average 1.2 sodium ion, compared to the total of 418 ions in the whole box. In AUT, a similar slab contains 4.7 chloride ions, compared to the total of 371. The anions diffuse easier from the AUT surface than the cations from the MUA surface, resulting in slight polarization of the water. This is manifested in a subtle preference of the bulk water above AUT, to orient along the z direction. Although this effect is very small, it can be important for example for orientation of a protein bound to the SAM surface. Similar behaviour of water in contact with a monolayer has been observed in case of a lipid bilayer. Åman et al. have simulated a bilayer of dipalmitoylphosphatidycholine interfaced with water [39]. A region of decreased density of water has been observed next to the bilayer surface. It has been observed that within the volume of water affected by the lipid layer, the molecules are oriented and this orientation changes along the normal vector of the layer (the order parameter changes the sign). Therefore, it is notable, how well a self-assembled monolayer of alkanethiols attached to the gold surface can mimic a biological membrane.

To check how much the results are affected by applying PBC in the z direction, another simulation of AUT has been designed (AUT2), with a box significantly elongated in the z direction (initial length was set to 200 Å), in order to minimize the artefacts arising from

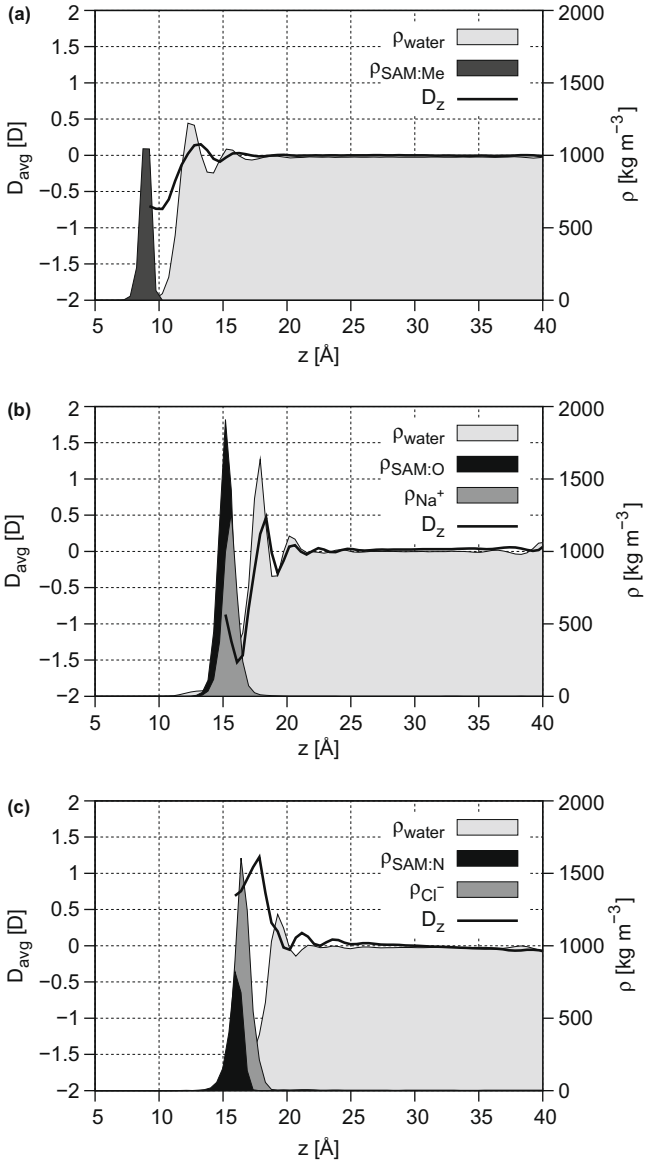

Fig. 4. Density profiles of water, ions (Na^+ and Cl^-) and terminal groups of SAM (SAM:Me – methyl group of HXT, SAM:O – carboxyl oxygens of MUA, SAM:N – nitrogen of AUT) plotted along the z axis, which is perpendicular to the SAM; D_z component of the dipole moment of water averaged to a single molecule of water; (a) HXT, (b) MUA, (c) AUT.

the use of PBC. The densities of the bulk water over the SAMs of HXT, MUA and AUT seem to be slightly overestimated; the density of water in the HXT simulation box, averaged between $z = 20$ Å and $z = 40$ Å is 987 kg m^{-3} (996 with ions), whereas analogous simulation without the SAM gives the density of pure water 973 kg m^{-3} and the density of 0.15 M NaCl 980 kg m^{-3}. This means that the density is overestimated by ca. 1.5%. Density of water in the MUA model, averaged between $z = 25$ Å and $z = 35$ Å is 998 kg m^{-3}—overestimated by ca. 1.2%. This increase is not a physical effect, but merely an artefact stemming from the application of PBC: it seems, that despite the 50 Å separation between the images of SAM, there is still some long-range interaction, which causes a contraction of the system along the direction perpendicular to the surface, resulting in turn in an increased density of water. Comparison of the two models of AUT, one 50 Å high (AUT) and other 200 Å high (AUT2), shows that the bulk water in the first one has the density of 988 kg m^{-3} whereas in the second model, the density of bulk water is 970 kg m^{-3}. Despite the fact that the density is slightly overestimated, the shape of the

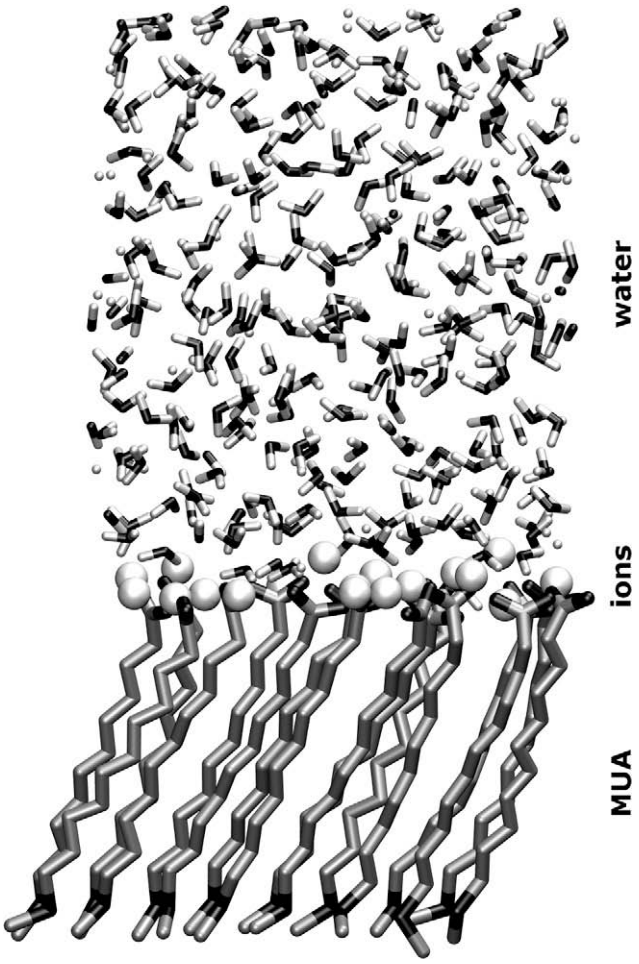

Fig. 5. Fragment of the interface between MUA and water: sodium cations form a stable layer on top of the SAM.

profile is preserved and therefore all the conclusions drawn from the models of HXT, MUA and AUT are still valid. The same stands for the D_z profile—which has the same shape regardless of the size of the box in the z direction.

4. Conclusions

Simulations of selected types of SAMs were performed at a pH that guarantees neutral, positively and negatively charged surfaces, depending on the functional groups. Tilt angles of the monolayer are in the range 21° (AUT) to 26° (MUA). The molecules are arranged into different configurations: HXT, which has the shortest chain, adopts NN configuration, MUA is in NNN configuration, whereas AUT adopts configuration between NN and NNN position. For charged SAMs, the counterions form a stable layer on top of the SAM and the density profile of the ions overlaps with the density profile of SAM, meaning that the ions are also bound between the terminal groups. In each case, a gap between SAM and solvent was observed, but it was found to be largest in HXT. The water at the interface has a layered structure, where the first layer has significantly increased density (up to 160% in MUA) and definite orientation, as seen in the averaged dipole moment. Although the increase in the density seems to be enormous, it has to be emphasized that it is a local effect, resulting from the ordering of water molecules into layers. The density and the dipole moment diminish in an oscillatory manner, when going from the interface into bulk water. The interactions with SAM have relatively long range: although the density reaches the bulk value within ca. 5 Å from the interface, the separation between periodic images of SAM in the simulation box has to be at least 50 Å; otherwise the water is "squeezed" by interacting images of SAM. At 50 Å separation, the density of water may be still overestimated by 1–2%. This is an important observation and has to be taken into consideration, when constructing the models of periodic monolayers.

Acknowledgements

The work was supported by a fellowship no. SFRH/BPD/38809/2007 awarded to B.S. by Fundação para a Ciência e a Tecnologia, Lisbon, Portugal. Calculations were performed at Wrocław Centre for Networking and Supercomputing (WCSS), Wrocław, Poland.

References

[1] J.C. Love, L.A. Estroff, J.K. Kriebel, R.G. Nuzzo, G.M. Whitesides, Chem. Rev. 105 (2005) 1103–1169.
[2] N.K. Chaki, K. Vijayamohanan, Biosens. Bioel. 17 (1-2) (2002) 1–12.
[3] E. Katz, I. Willner, Angew. Chem. Int. Ed. 43 (2004) 6042–6108.
[4] G. Heimel, L. Romaner, E. Zojer, J.-L. Bredas, Acc. Chem. Res. 41 (2008) 721–729.
[5] P. Ghosh, G. Han, M. De, C.K. Kim, V.M. Rotello, Adv. Drug Deliv. Rev. 60 (11) (2008) 1307–1315.
[6] M.J. Stevens, G.S. Grest, Biointerphases 3 (2008) 13–22.
[7] V. Ostroverkhov, G.A. Waychunas, Y.R. Shen, Phys. Rev. Lett. 94 (4) (2005) 046102.
[8] M.D. Porter, T.B. Bright, D.L. Allara, C.E.D. Chidsey, J. Am. Chem. Soc. 109 (1987) 3559–3568.
[9] S. Balasubramanian, M.L. Klein, J.I. Siepmann, J. Chem. Phys. 103 (1995) 3184–3194.
[10] F.S. Damos, R.C.S. Luz, L.T. Kubota, Langmuir 21 (2005) 602–609.
[11] D. Schwendel, T. Hayashi, R. Dahint, A. Pertsin, M. Grunze, R. Steitz, F. Shreiber, Langmuir 19 (2003) 2284–2293.
[12] C.E.D. Chidsey, D.N. Loiacono, Langmuir 6 (1990) 682–691.
[13] N. Winter, J. Vieceli, I. Benjamin, J. Phys. Chem. B 112 (2008) 227–231.
[14] K.P. Fears, S.E. Creager, R.A. Latour, Langmuir 24 (2008) 837–843.
[15] B. Szefczyk, M.N.D.S. Cordeiro, R. Franco, J.A.N.F. Gomes, J. Biol. Inorg. Chem. 14 (2009) 1119–1128.
[16] T. Hayashi, Y. Moricawa, H. Nozoye, J. Phys. Chem. 114 (17) (2001) 7615–7621.
[17] M.C. Vargas, P. Giannozzi, A. Selloni, C. Scoles, J. Phys. Chem. B 105 (39) (2001) 9509–9513.
[18] M.L. Carot, V.A. Macagno, P. Paredes-Oliveira, E.M. Patrito, J. Phys. Chem. C 111 (2007) 4294–4304.
[19] F. Tielens, D. Costa, V. Humblot, C.-M. Pradier, J. Phys. Chem. C 112 (2008) 182–190.
[20] H. Kondoh, M. Iwasaki, T. Shimada, K. Amemiya, T. Yokoyama, T. Ohta, M. Shimomura, S. Kono, Phys. Rev. Lett. 90 (6) (2003) 066102.
[21] M.G. Roper, M.P. Skegg, C.J. Fisher, J.J. Lee, V.R. Dhanak, D.P. Woodruff, R.G. Jones, Chem. Phys. Lett. 389 (1-3) (2004) 87–91.
[22] R. Mazzarello, A. Cossaro, A. Verdini, R. Rousseau, L. Casalis, M.F. Danisman, L. Floreano, S. Scandolo, A. Morgante, G. Scoles, Phys. Rev. Lett. 98 (2007) 016102.
[23] A. Cossaro, R. Mazzarello, R. Rousseau, L. Casalis, A. Verdini, A. Kohlmeyer, L. Floreano, S. Scandolo, A. Morgante, M.L. Klein, G. Scoles, Science 321 (2008) 943–946.
[24] W.F. van Gunsteren, S.R. Billeter, A.A. Eising, P.H. Hünenberger, P. Krüger, A.E. Mark, W.R.P. Scott, I.G. Tironi, Biomolecular Simulation: The GROMOS96 manual and user guide, Hochschulverlag AG an der ETH Zürich, Zürich, Switzerland, 1996.
[25] W. Mar, M.L. Klein, Langmuir 10 (1994) 188–196.
[26] H.J.C. Berendsen, J.P.M. Postma, W.F. van Gunsteren, J. Hermans, Interaction models for water in relation to protein hydration, in: B. Pullman (Ed.), Intermolecular Forces, D. Reidel Publishing Company, Dordrecht, 1981, pp. 331–342.
[27] B. Hess, C. Kutzner, D. van der Spoel, E. Lindahl, J. Chem. Theory Comput. 4 (2008) 435447.
[28] S. Nosé, Mol. Phys. 52 (1984) 255–268.
[29] W.G. Hoover, Phys. Rev. A 31 (1985) 1695–1697.
[30] M. Parrinello, A. Rahman, J. Appl. Phys. 52 (1981) 7182–7190.
[31] B. Hess, H. Bekker, H.J.C. Berendsen, J.G.E.M. Fraaije, J. Comp. Chem. 18 (1997) 1463–1472.
[32] S.V. Merzlikin, N.N. Tolkachev, T. Strunskus, G. Witte, T. Glogowski, C. Wöll, W. Grünert, Surf. Sci. 602 (2008) 755–767.
[33] C.D. Bain, E.B. Troughton, Y.-T. Tao, J. Evall, G.M. Whitesides, R.G. Nuzzo, J. Am. Chem. Soc. 111 (1989) 321–335.
[34] V. Bindu, T. Pradeep, Vacuum 49 (1998) 63–66.
[35] D.M. Duffy, J.H. Harding, Langmuir 21 (2005) 3850–3857.
[36] R. Bhatia, B.J. Garrison, Langmuir 13 (1997) 4038–4043.
[37] U.K. Sur, V. Lakshminarayanan, J. Colloid. Interface Sci. 254 (2002) 410–413.
[38] A.J. Pertsin, T. Hayashi, M. Grunze, J. Phys. Chem. B 106 (2002) 12274–12281.
[39] K. Åman, E. Lindahl, O. Edholm, P. Håkansson, P.-O. Westlund, Biophys. J. 84 (2003) 102–115.